

Stabilized 14.0%-efficient triple-junction thin-film silicon solar cell

Hitoshi Sai (齋均), Takuya Matsui (松井卓矢), and Koji Matsubara (松原浩司)

Citation: [Appl. Phys. Lett.](#) **109**, 183506 (2016);

View online: <https://doi.org/10.1063/1.4966996>

View Table of Contents: <http://aip.scitation.org/toc/apl/109/18>

Published by the [American Institute of Physics](#)

Articles you may be interested in

[Triple-junction thin-film silicon solar cell fabricated on periodically textured substrate with a stabilized efficiency of 13.6%](#)

[Applied Physics Letters](#) **106**, 213902 (2015); 10.1063/1.4921794

[Amorphous silicon solar cell](#)

[Applied Physics Letters](#) **28**, 671 (2008); 10.1063/1.88617

[High-efficiency amorphous silicon solar cells: Impact of deposition rate on metastability](#)

[Applied Physics Letters](#) **106**, 053901 (2015); 10.1063/1.4907001

[A 2-terminal perovskite/silicon multijunction solar cell enabled by a silicon tunnel junction](#)

[Applied Physics Letters](#) **106**, 121105 (2015); 10.1063/1.4914179

[19.8% efficient "honeycomb" textured multicrystalline and 24.4% monocrystalline silicon solar cells](#)

[Applied Physics Letters](#) **73**, 1991 (1998); 10.1063/1.122345

[Reversible conductivity changes in discharge-produced amorphous Si](#)

[Applied Physics Letters](#) **31**, 292 (2008); 10.1063/1.89674



5 Electronic Measurement Pitfalls to Avoid

Get the whitepaper

Stabilized 14.0%-efficient triple-junction thin-film silicon solar cell

Hitoshi Sai (齋均),^{a)} Takuya Matsui (松井卓矢), and Koji Matsubara (松原浩司)

Research Center for Photovoltaics, National Institute of Advanced Industrial Science and Technology (AIST), Central 2, Umezono 1-1-1, Tsukuba, Ibaraki 305-8568, Japan

(Received 8 September 2016; accepted 17 October 2016; published online 1 November 2016)

We report on a high-efficiency triple-junction thin-film silicon solar cell fabricated using the substrate configuration. An undoped hydrogenated amorphous silicon (a-Si:H) solar cell grown using triode plasma-enhanced chemical vapor deposition, which is more stable against light soaking, was applied to the a-Si:H/ μ c-Si:H/ μ c-Si:H triple-junction cells with honeycomb-textured substrates. To find the best balance in short circuit density and fill factor, we quantitatively investigated the effect of current mismatch on triple-junction cells. Accordingly, a stabilized efficiency of 14.04% was achieved in an a-Si:H/ μ c-Si:H/ μ c-Si:H triple-junction solar cell with a minimum light-induced degradation of 4%, setting a new record in this type of solar cells. *Published by AIP Publishing.*

[<http://dx.doi.org/10.1063/1.4966996>]

Thin-film silicon solar cells (TFSSCs) based on plasma-enhanced chemical vapor deposition (PECVD) have been used in a wide variety of applications ranging from large-area photovoltaic systems to consumer products, including light-weight flexible solar cells on plastic substrates, owing to their relatively low growth temperature ($\sim 200^\circ\text{C}$).^{1,2} The main aim of TFSSCs is to improve the power-conversion efficiency. It is well known that the efficiency of hydrogenated amorphous silicon (a-Si:H) solar cells with a typical bandgap energy of 1.7 eV degrades by 10%–20% after a prolonged exposure to light,³ which is known as the Staebler–Wronski effect.⁴ This detrimental effect has been impeding the improvement of efficiency until now. Compared to the pure amorphous materials, hydrogenated microcrystalline silicon (μ c-Si:H) with an E_g of 1.1 eV has higher tolerance to light soaking.⁵ Therefore, the multi-junction approach using a stack of a-Si:H and μ c-Si:H cells is an effective way to mitigate light-induced degradation and to improve stabilized efficiency.^{6–9} To date, a record stabilized efficiency of 13.6% was realized in a substrate-type a-Si:H/ μ c-Si:H/ μ c-Si:H triple-junction cell.⁹ In this triple-junction cell, periodically textured substrates play a key role to enhance light absorption within the μ c-Si:H subcells.^{10,11} However, there is large room for improvement especially in the a-Si:H top cell and the current matching among the subcells.⁹ In this study, we have attempted to improve these aspects. Initially, the triode PECVD technique, which enables us to grow a relatively stable a-Si:H material,^{7,12} was applied to the substrate-type a-Si:H solar cells. The light-induced degradation behavior in these cells was investigated. Then, the triode PECVD-based a-Si:H cells were incorporated into the triple-junction cells. The impact of current mismatches in the triple-junction cells on photovoltaic performances was also investigated. Finally, we reported a stabilized efficiency of 14.04% in an a-Si:H/ μ c-Si:H/ μ c-Si:H triple-junction solar cell, thus setting a new record.

Throughout this study, we focus on TFSSCs with a substrate configuration. Two types of substrates were prepared: commercial SnO_2 :F-coated glass substrates and periodically textured substrates with a hexagonal dimple array, which is referred as “honeycomb-textured substrates.” The former was used for developing single-junction a-Si:H cells, whereas the latter was used for fabricating triple-junction cells. The details of the fabrication procedure of honeycomb-textured substrates were reported elsewhere.^{10,11} Before the growth of the Si film, both substrates were coated with the Ag and ZnO:Ga (GZO) films to obtain a highly conductive and reflective surface. All the Si-related layers including *p*- and *n*-type doped layers were grown with PECVD at temperatures in the range 140–200 °C, using SiH_4 , H_2 , B_2H_6 , PH_3 , and CO_2 as source gases. Most of the layers were grown using a laboratory-scale PECVD with the exception of undoped μ c-Si:H layers, which were grown using a large-scale very-high-frequency (VHF) PECVD.^{13,14} Undoped a-Si:H layers were grown at a deposition rate (DR) of 0.03 nm/s using a triode PECVD reactor (60 MHz), in which a mesh electrode was placed between the powered and grounded electrodes.⁷ As a reference material, the a-Si:H films were deposited by the standard diode PECVD system (13.56 MHz) at a DR of 0.08 nm/s, using a minimum power density to sustain plasma discharge in this system. After the PECVD processes, the transparent conductive oxide (TCO) films of In_2O_3 :Sn (ITO) or In_2O_3 :H (IOH)¹⁵ were deposited as a front window electrode using a radio frequency (RF) magnetron sputtering at room temperature followed by a post-annealing process at 175 °C. In the case of triple-junction cells, cell isolation was also performed using reactive ion etching before the post-annealing process.

The cell performance was evaluated by measuring the current density–voltage (*J*–*V*) characteristics under air mass 1.5G (100 mW/cm²), using a dual-light solar simulator (Wacom Electric, WXS-50S-L2). The open-circuit voltage (V_{OC}), short-circuit current density (J_{SC}), fill factor (FF), and efficiency were also recorded. External quantum efficiency (EQE) spectra were measured with a Bunkou-Keiki, CEP-25BXS setup. For some solar cells, an antireflection (AR) film based on the moth-eye structure¹⁶ was applied to suppress the

^{a)} Author to whom correspondence should be addressed. Electronic mail: hitoshi-sai@aist.go.jp

reflection loss. Light soaking of solar cells was performed under the standard condition (1 Sun at 50 °C for 1000 h). For some experiments, an accelerated light soaking (3 Sun at 60 °C for 6 h) was also used.

Figure 1 shows the J - V curves of two typical substrate-type a-Si:H solar cells grown with the diode and triode PECVD techniques before and after light soaking under the accelerated condition. Photovoltaic parameters of the cells are also summarized in this figure. The device structure used is textured as a $\text{SnO}_2/\text{Ag}/\text{GZO}/(\text{n})\text{a-Si:H}/(\text{i})\text{a-Si:H}(t_i = 250 \text{ nm}, \text{diode or triode})/\text{buffer}/(\text{p})\text{nc-SiO}_x/\text{H}/\text{ITO}/\text{Ag}$ grid from the bottom to the top. The oxygen content of the (p)nc-SiO_x:H layer¹⁶ was increased from that used in the previous report⁹ for improving V_{OC} and reducing absorption loss. The i-p buffer layer was also modified accordingly to adapt to the increased oxygen content in the p-layer. The details would be reported elsewhere. As seen in Fig. 1, the two solar cells show almost identical parameters in the initial state. However, after light soaking, degradation in FF is largely mitigated using triode PECVD. As a result, a relatively high stabilized efficiency of 9.2% was achieved with an active area of 0.25 cm². The efficiency degradation in this cell ($\Delta 10.9\%$) is notably small, which agrees well with the previous report using the superstrate-type a-Si:H cells.¹²

The triode PECVD was applied to the substrate-type a-Si:H/ $\mu\text{c-Si:H}/\mu\text{c-Si:H}$ triple-junction cells. Figure 2 shows a cross-sectional transmission electron microscope image of a typical triple-junction cell fabricated in this study, using a honeycomb-textured substrate with a texture period of 4 μm . The device structure is as follows: honeycomb-textured substrate/Ag/GZO/bottom $\mu\text{c-Si:H}$ cell/middle $\mu\text{c-Si:H}$ cell/top a-Si:H cell(triode or diode)/IOH/Ag grid, from the bottom to the top. Each $\mu\text{c-Si:H}$ cell is a stack of (n) $\mu\text{c-Si:H}/(\text{n})\text{nc-SiO}_x/(\text{i})\mu\text{c-Si:H}/(\text{p})\text{nc-SiO}_x/(\text{p})\mu\text{c-Si:H}$. The upper most (p) $\mu\text{c-Si:H}$ layers are expected to contribute to the realization of good tunnel junctions between the subcells.¹⁷ The total thickness of the Si-based layers is approximately 4 μm , and the thickness of the active layers in the top, middle, and bottom cells is 0.23 μm , 1.6 μm , and 1.8 μm , respectively. It is observed in Fig. 2 that these thicknesses are not uniform over the cell and become thinner by a maximum of $\sim 15\%$ at

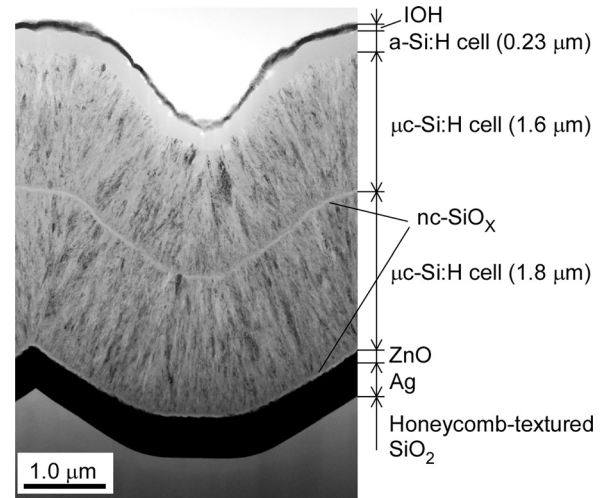


FIG. 2. Cross-sectional TEM image of a substrate-type a-Si:H/ $\mu\text{c-Si:H}/\mu\text{c-Si:H}$ triple-junction cell fabricated in this study.

the concave of the honeycomb textures, owing to the shadow effect during the PECVD process.¹⁸

As shown in Fig. 1, FF is an efficient measure to evaluate light-induced degradation in a-Si:H cells. Therefore, we compare the FF in triple-junction cells that have a-Si:H top cells grown using the diode or triode PECVD. Figure 3 shows the variation of the FF in triple-junction cells before and after light soaking under the standard condition. The distribution in the initial FF is mainly attributed to the difference in the current mismatches among the subcells. The low initial FFs shown here ($\text{FF}(\text{Ini}) < 0.76$) correspond to the cells with a very small current mismatch (almost balanced) or a weakly top-cell limited condition. As a reference, a solid line corresponding to no degradation ($\text{FF}(\text{LS}) = \text{FF}(\text{Ini})$) is also plotted. It is found in Fig. 3 that FF is deteriorated after light soaking by 3%–6%, but the degradation is rather mitigated compared to the single-junction a-Si:H cells, owing to the configuration of triple-junction. The cells fabricated with

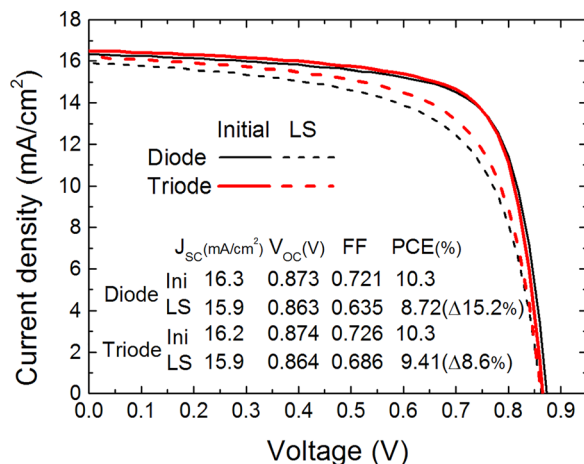


FIG. 1. J - V curves of substrate-type a-Si:H solar cells grown using the diode and triode PECVD techniques before and after light soaking (LS) under the accelerated condition (3 Sun at 60 °C for 6 h).

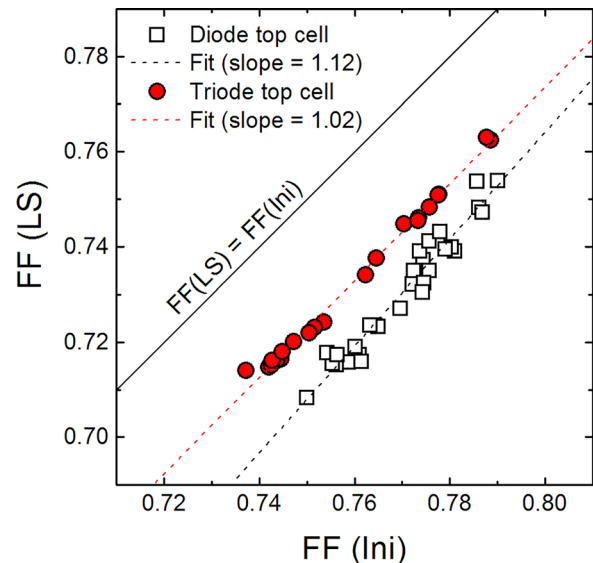


FIG. 3. Comparison of FF in triple-junction cells in the initial state (Ini) and after light soaking (LS). Light soaking was performed under the standard condition. Dashed lines show the linear fits of the experimental data.

triode PECVD show less degradation (3%–4%) than those with diode PECVD (4.5%–6%) over the entire range, as indicated in Fig. 3. It is also found that the slope of the linear fit line for the triode case (slope = 1.02) is smaller than the diode case (1.12), showing that the former shows a higher tolerance to light soaking especially in the case of lower initial FF—in other words, under or closer to the top-limited condition. These results clearly indicate that triode PECVD contributes to mitigate the light-induced degradation even in triple-junction cells.

The current matching among subcells is an important aspect to realize high-efficiency multi-junction TFSSCs. In general, J_{SC} is maximized by realizing a perfect current matching among all subcells, whereas the FF increases when the current mismatch increases. Thus, there is a trade-off between J_{SC} and FF linked to current matching. In addition, light-induced degradation in a-Si:H cells, which causes a reduction in J_{SC} and FF, as shown in Fig. 1, is taken into account for realizing a higher stabilized efficiency. In the case of a-Si:H/ μ c-Si:H tandem solar cells, limiting the current density by the bottom μ c-Si:H cell, which in general shows higher FF than the other after light soaking, leads to a higher stabilized efficiency.^{19,20} Similarly, limiting the current density by the middle or bottom μ c-Si:H cell is expected to be beneficial in the a-Si:H/ μ c-Si:H/ μ c-Si:H triple-junction cells.

Figure 4 shows the variations in J_{SC} , V_{OC} , and FF and efficiency of a-Si:H/ μ c-Si:H/ μ c-Si:H triple-junction cells with different top cell thicknesses (0.23–0.25 μ m) before and after light soaking under the accelerated condition. All the top a-Si:H cells were fabricated with triode PECVD. Here, the x-axis shows the current mismatch with respect to the top a-Si:H cell:

$$\Delta J_{TOP} = J_{TOP} - J_{MID} \text{ for } J_{MID} \leq J_{BOT},$$

$$\Delta J_{TOP} = J_{TOP} - J_{BOT} \text{ for } J_{MID} > J_{BOT},$$

where J_{TOP} , J_{MID} , and J_{BOT} are the top, middle, and bottom subcell current densities calculated from EQE spectra, respectively. In this figure, the triple-junction cells are categorized into two groups according to their ΔJ_{TOP} before light soaking: (A) $\Delta J_{TOP} > 1.0 \text{ mA/cm}^2$ (strongly middle- or bottom-limited) and (B) $\Delta J_{TOP} < 1.0 \text{ mA/cm}^2$ (almost balanced). As shown in Fig. 4(a), J_{SC} increases monotonically with a decrease in ΔJ_{TOP} . After light soaking, ΔJ_{TOP} tends to decrease because of the light-induced degradation in the a-Si:H top cells and some of the cells fall into the top-limited condition with negative ΔJ_{TOP} . On the contrary, the highest FF is obtained in the cells with large ΔJ_{TOP} (group A), as shown in Fig. 4(c). This tendency is maintained even after light soaking. It is also found that the highly mismatched cells (group A) show a slightly smaller degradation (averaged $\Delta FF = -2.6\%$) than the others (-3.1%). In contrast to J_{SC} and FF, V_{OC} is almost independent of ΔJ_{TOP} and light-soaking treatment, as shown in Fig. 4(b). As a result of these variations, the highest stabilized efficiency of 13.9% is obtained in group A, which possesses positive ΔJ_{TOP} after light soaking, as shown in Fig. 4(d). It should be pointed out that J_{SC} in group B does not decrease by light soaking significantly, even with the negative ΔJ_{TOP} (top-limited), as shown in Fig. 4(b). We attribute this to the slightly blue-rich spectrum of our dual-light solar simulator, which causes a slight overestimation of J_{SC} for top-limited cells. However, we confirmed that this effect is rather minor and does not change the general trends observed in Fig. 4.

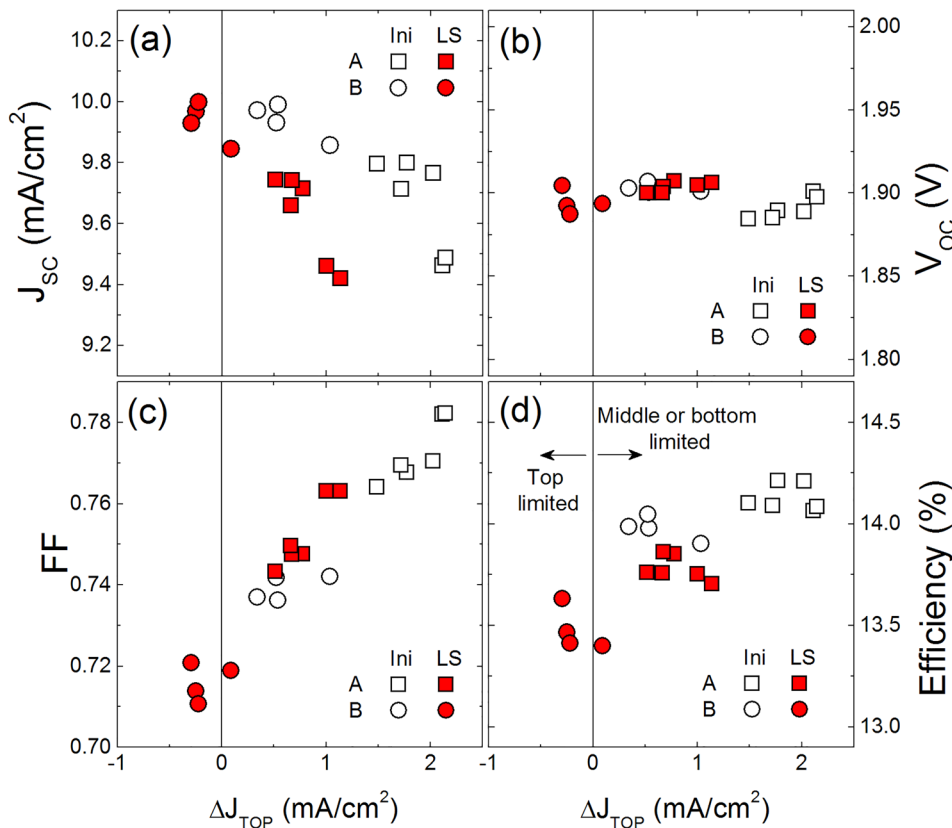
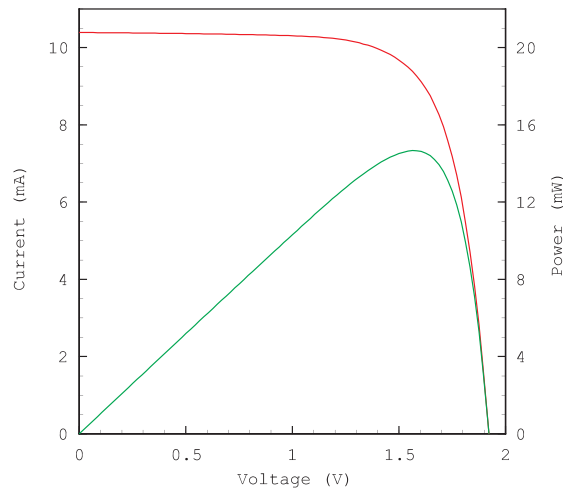


FIG. 4. Photovoltaic parameters of a-Si:H/ μ c-Si:H/ μ c-Si:H triple-junction cells in the initial state (Ini) and after light soaking (LS) as a function of current mismatch with respect to the top a-Si:H cell, ΔJ_{TOP} . Light soaking was performed under the accelerated condition (3 Sun at 60 °C for 6 h). J_{SC} and efficiency were evaluated using an active area of 1.06 cm^2 without AR films.

I-V CURVE
IEC60904-3Ed.2 1.045 cm² (designated area) WHSS



Date : 26 May 2016
Data No : SC2510A1-01
Sample No : SC2510A1
Repeat Times : 5

I_{sc} 10.39 mA
 V_{oc} 1.922 V
 P_{max} 14.67 mW
 I_{pmax} 9.38 mA
 V_{pmax} 1.563 V
F.F. 73.4 %
Eff (da) 14.04 %
DTemp. 25.0 °C
MTemp. 24.9 °C
D Irr. 100.0 mW/cm²
M Irr. 99.4 mW/cm² (top)
100.8 mW/cm² (middle)
100.2 mW/cm² (bottom)

Scan Mode
Isc to Voc

FIG. 5. *I*-*V* curve of the record a-Si:H/ μ c-Si:H/ μ c-Si:H triple-junction solar cell independently confirmed by the AIST CSM team.



TABLE I. Independently confirmed photovoltaic parameters of the new and previous record efficiency triple-junction cells after light soaking under 1 Sun at 50 °C for 1000 h.

ID	J_{sc} (mA/cm ²)	V_{oc} (V)	FF	Stabilized efficiency (%)
SC2510 (this study)	9.94	1.922	0.734	14.04
SC1913 ⁹	9.92	1.901	0.721	13.60

A series of triple-junction cells were fabricated with careful attention to the current matching, taking into account the aforementioned findings. Some of the promising cells were evaluated with an AR film followed by light soaking under the standard conditions. The best efficiency cell obtained showed initial and stabilized efficiencies of 14.5% and 13.9%, respectively, with a very small efficiency degradation of 4%. This cell was subsequently sent to the Characterization, Standard and Measurement team of the Research Center for Photovoltaics, National Institute of Advanced Industrial Science and Technology (AIST CSM team), and a stabilized efficiency of 14.04% has been independently confirmed with a designated area (da) of

1.045 cm², as shown in Fig. 5. This value is higher than the current record stabilized efficiency reported so far (13.60%),⁹ setting a new world record for TFSSCs. Photovoltaic parameters of these two stabilized solar cells are compared in Table I. It is found that the improvements in V_{oc} ($\sim 1\%$) and FF ($\sim 2\%$) contribute to the total efficiency gain ($\sim 3\%$). The gain in FF should be ascribed to the more stable a-Si:H top cell and the proper current-matching design. As shown in Fig. 6, the new record cell shows subcell current densities of (J_{TOP} , J_{MID} , J_{BOT}) = (11.2, 10.0, 10.2) mA/cm² with a large ΔJ_{TOP} = 1.2 mA/cm², which is beneficial to obtain a higher FF. In contrast, in the previous record, ΔJ_{TOP} is only 0.4 mA/cm² with a large surplus current density in the bottom cell ((J_{TOP} , J_{MID} , J_{BOT}) = (10.3, 9.9, 11.1) mA/cm²).⁹ The origin of the V_{oc} gain is not sufficiently clear, but we expect that the optimized buffer and p-layer in the top a-Si:H cell contribute to this to some extent.

In summary, stable a-Si:H cells grown using triode PECVD were applied to the substrate-type a-Si:H/ μ c-Si:H/ μ c-Si:H triple-junction cells. The effect of current mismatch on triple-junction cells was investigated quantitatively to find the best balance for realizing highly stabilized efficiency after prolonged light soaking. Accordingly, a stabilized efficiency of 14.04% was independently confirmed by the AIST CSM team with a minimum efficiency degradation of 4%, thus setting a new record. It should be pointed out that the substrate-type a-Si:H top cell developed in this study is still less efficient compared with the record of a-Si:H cell with the superstrate configuration.⁷ Further improvement in efficiency is expected by tackling this issue.

The authors acknowledge Dr. Hishikawa and Ms. Sasaki of AIST CSM team for the precise measurements of solar cells and Mr. Miyagi, Sato, Kumagai, Fukuju, and Ms. Tanabe for their technical support for this work. A part of this work was supported by the Photovoltaic Power Generation Technology Research Association (PVTEC) and the New Energy and Industrial Technology Development Organization (NEDO), Japan.

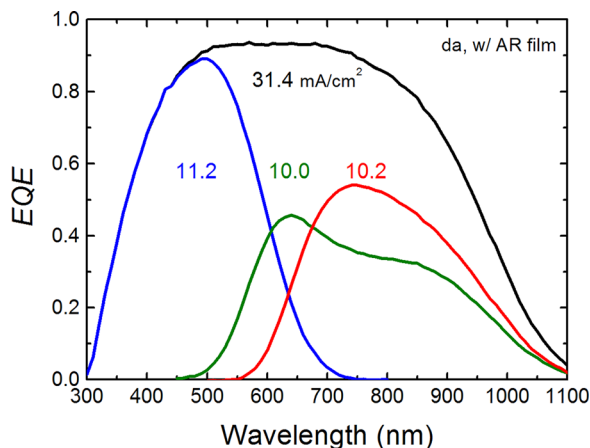


FIG. 6. EQE spectra of the new record efficiency triple-junction cell after light soaking. An AR film was attached on the top of the cell.

- ¹M. N. van den Donker, A. Gordijn, H. Stiebig, F. Finger, B. Rech, B. Stannowski, R. Bartl, E. A. G. Hamers, R. Schlatmann, and G. J. Jongerden, *Sol. Energy Mater. Sol. Cells* **91**, 572 (2007).
- ²B. Yan, J. Yang, and S. Guha, *J. Vac. Sci. Technol., A* **30**, 04D108 (2012).
- ³M. Stuckelberger, M. Despeisse, G. Bugnon, J.-W. Schüttai, F.-J. Haug, and C. Ballif, *J. Appl. Phys.* **114**, 154509 (2013).
- ⁴D. L. Staebler and C. R. Wronski, *Appl. Phys. Lett.* **31**, 292 (1977).
- ⁵J. Meier, R. Flückiger, H. Keppner, and A. Shah, *Appl. Phys. Lett.* **65**, 860 (1994).
- ⁶M. Boccard, M. Despeisse, J. Escarre, X. Niquille, G. Bugnon, S. Hänni, M. Bonnet-Eymard, F. Meillaud, and C. Ballif, *IEEE J. Photovoltaics* **4**, 1368 (2014).
- ⁷T. Matsui, K. Maejima, A. Bidiville, H. Sai, T. Koida, T. Suezaki, M. Matsumoto, K. Saito, I. Yoshida, and M. Kondo, *Jpn. J. Appl. Phys., Part 1* **54**, 08KB10 (2015).
- ⁸S. Kim, J.-W. Chung, H. Lee, J. Park, Y. Heo, and H.-M. Lee, *Sol. Energy Mater. Sol. Cells* **119**, 26 (2013).
- ⁹H. Sai, T. Matsui, T. Koida, K. Matsubara, M. Kondo, S. Sugiyama, H. Katayama, Y. Takeuchi, and I. Yoshida, *Appl. Phys. Lett.* **106**, 213902 (2015).
- ¹⁰H. Sai, K. Saito, and M. Kondo, *Appl. Phys. Lett.* **101**, 173901 (2012).
- ¹¹H. Sai, K. Saito, N. Hozuki, and M. Kondo, *Appl. Phys. Lett.* **102**, 053509 (2013).
- ¹²T. Matsui, A. Bidiville, K. Maejima, H. Sai, T. Koida, T. Suezaki, M. Matsumoto, K. Saito, I. Yoshida, and M. Kondo, *Appl. Phys. Lett.* **106**, 053901 (2015).
- ¹³H. Sai, K. Maejima, T. Matsui, T. Koida, M. Kondo, S. Nakao, T. Takeuchi, H. Katayama, and I. Yoshida, *Jpn. J. Appl. Phys., Part 1* **54**, 08KB05 (2015).
- ¹⁴T. Koida, H. Fujiwara, and M. Kondo, *Jpn. J. Appl. Phys., Part 2* **46**, L685 (2007).
- ¹⁵H. Sai, T. Matsui, K. Saito, M. Kondo, and I. Yoshida, *Prog. Photovoltaics: Res. Appl.* **23**, 1572 (2015).
- ¹⁶R. Biron, C. Pahud, F.-J. Haug, J. Escarré, K. Söderström, and C. Ballif, *J. Appl. Phys.* **110**, 124511 (2011).
- ¹⁷A. Banerjee, J. Yang, T. Glattelter, K. Hofman, and S. Guha, *Appl. Phys. Lett.* **64**, 1517 (1994).
- ¹⁸H. Sai, T. Koida, T. Matsui, I. Yoshida, K. Saito, and M. Kondo, *Appl. Phys. Express* **6**, 104101 (2013).
- ¹⁹M. Bonnet-Eymard, M. Boccard, G. Bugnon, F. Sculati-Meillaud, M. Despeisse, and C. Ballif, *Sol. Energy Mater. Sol. Cells* **117**, 120 (2013).
- ²⁰B. Blank, C. Ulbrich, T. Merdzhanova, C. Zahren, B. E. Pieters, A. Gerber, and U. Rau, *Sol. Energy Mater. Sol. Cells* **143**, 1 (2015).